LLNL-JRNL-520653

LAWRENCE
LIVERMORE
NATIONAL
LABORATORY

Tailored ramp loading via shock release of stepped density reservoirs

S. T. Prisbrey, H. S. Park, B. A. Remington, R. Cavallo, M. May, S. M. Pollaine, R. Rudd, B. Maddox, L. Fried, K. Blobaum, R. Wallace, M. Wilson, D. Swift, J. Satcher, T. Perry, A. Comley, E. Giraldez, M. Farrel, A. Nikroo

December 19, 2011

Physics of Plasmas

Disclaimer

This document was prepared as an account of work sponsored by an agency of the United States government. Neither the United States government nor Lawrence Livermore National Security, LLC, nor any of their employees makes any warranty, expressed or implied, or assumes any legal liability or responsibility for the accuracy, completeness, or usefulness of any information, apparatus, product, or process disclosed, or represents that its use would not infringe privately owned rights. Reference herein to any specific commercial product, process, or service by trade name, trademark, manufacturer, or otherwise does not necessarily constitute or imply its endorsement, recommendation, or favoring by the United States government or Lawrence Livermore National Security, LLC. The views and opinions of authors expressed herein do not necessarily state or reflect those of the United States government or Lawrence Livermore National Security, LLC, and shall not be used for advertising or product endorsement purposes.

Tailored ramp-loading via shock release of stepped-density reservoirs

Shon T. Prisbrey, Hye-Sook Park, Bruce A. Remington, Robert Cavallo, Mark May, Stephen M. Pollaine, Robert Rudd, Brian Maddox, Andrew Comley, Larry Fried, Kerri Blobaum, Russ Wallace, Mike Wilson, David Swift, Joe Satcher, Ted Perry

Lawrence Livermore National Laboratory, 7000 East Avenue, Livermore CA, 94550, USA

Emilio Giraldez, Michael Farrell, Abbas Nikroo

General Atomics, San Diego, California 92186, USA

Abstract

The concept of a gradient piston drive has been extended from that of a single component reservoir, such as a high explosive, to that of a multi-component reservoir that utilizes low density foams and large shocks to achieve high pressures (~ 3.5 Mbar) and controlled pressure vs. time profiles on a driven sample. Simulated and experimental drives shaped through the use of multiple component (including carbonized resorcinol formaldehyde and SiO_2 foam) reservoirs are compared. Individual density layers in a multiple component reservoir are shown to correlate with velocity features in the measured drive which enables the ability to tune a pressure drive by adjusting the components of the reservoir. Pre-shot simulations are shown to be in rough agreement with data but post-shot simulations involving the use of simulated plasma drives were needed to achieve an exact match. Results from a multiple component reservoir shot (~3.5 Mbar) at the National Ignition Facility are shown.

Your manuscript has been submitted. Your manuscript tracking number is: POP37796DPP11B

I. INTRODUCTION

A large number of material and engineering fields need to access off-Hugoniot states to answer questions posed by systems or problems of study such as imploding diamond capsule shells for ICF ignition[1], asteroid impact on planetary bodies, and high strain-rate deformation of solids[2]. In most – if not all – such cases the materials of interest are in a high pressure, low temperature region of phase space. As seen in Figure 1, such regions of phase space are not readily accessible via single shock experiments and, as a consequence, are not well characterized experimentally since an off-Hugoniot loading path is needed.

One method of off-Hugoniot loading was first proposed and demonstrated by Barnes et al[3] who utilized the stagnation of high-explosive by-products in an experiment to create quasi-isentropical compression on a rippled sample of aluminum. Within the last decade, this technique has been extended to the use of the plasma gradient piston which is produced by stagnation of a laser ablation-driven shock released by a thin[4] or thick[5] reservoir. Most recently, Park et al have shown that both direct laser ablation of a sample[6 7] and the use of hohlraums[8] to drive larger diameter samples can produce a plasma gradient piston of sufficient duration to allow for inference of material strength at pressures > 1 Mbar in V and Ta.

To better understand the use of a plasma gradient piston and its limitations it is useful to look at the physics of its generation and evolution. The pressure produced by the piston is primarily due to the ram pressure, ρu^2 (where ρ is the density and u is the velocity of the plasma flow), of the unloading material from the reservoir during stagnation (see Figure 2). For single component reservoirs where a large shock ionizes the releasing material into a gas, the resulting density, velocity, and pressure of the unloading material approach the self-similar solution given by Zel'dovich and Raizer[9] which are:

$$c = c_0 - \frac{\gamma - 1}{2}|u|, \qquad u < 0$$

$$\rho = \rho_o \left[1 - \frac{\gamma - 1}{2}\frac{|u|}{c_o}\right]^{2/(\gamma-1)}$$

$$p = p_o \left[1 - \frac{\gamma - 1}{2}\frac{|u|}{c_o}\right]^{2\gamma/(\gamma-1)}$$

$$|u| = \frac{2}{\gamma + 1}\left(c_o - \frac{x}{t}\right) \; and \; |u|_{max} = \frac{2}{\gamma - 1}c_o.$$

where c is the sound speed in the material, c_o is the sound speed in the shocked reservoir just prior to shock break out, γ is the polytropic index of the shocked material, and u, ρ, and p are velocity, density and pressure, respectively. For strong shocks, the releasing material is assumed to be a gas with constant γ which implies that the velocity as a function of position in the unloading material is a linear function of position and that the density of the unloading has a third order dependence on position. Since the form of the solution is self-similar, rise-times and peak pressure in an ideal plasma gradient piston drive will only be affected by changes is c_o and ρ_o for a fixed unloading distance (the effect of increasing or decreasing the strength of the unloading shock is reflected in c_o and ρ_o). From the equations, one can see that the temporal shape of a single density unloading reservoir is set by the strength of the initial shock and the unloading distance between the reservoir and the driven sample.

We show that the resultant plasma gradient piston drive profile can be controlled and tuned by changing the components of the unloading reservoir from that of a single component to one involving multiple components, i.e., one having differing c_o and ρ_o as a function of distance in the reservoir. As seen in Figure 2, the choice of densities and layer thicknesses are chosen to approximate the unloading profile of a single density layer. The use of multiple component reservoirs is beneficial in two ways: the distance needed between the back of the reservoir and the front of the sample is reduced, and individual pieces of the plasma piston drive profile can be adjusted through adjustment of the initial reservoir components. The reduction of the distance needed between the reservoir and the sample allows for the use of smaller experimental targets, specifically targets with dimensions that are feasible to use with laser-driven platforms. The ability to tune the individual pieces of the plasma piston drive means that the peak pressure in the drive can be increased by employing relatively thin, high-density layers in the reservoir

and, furthermore, that the lower density portion of the reservoir can be extended spatially beyond the limit set by the single-component self-similar solution to allow for a longer drive at lower pressure (which enables the use of samples that are thicker than the ~10 μm proposed by Edwards et al4).

Implied in the ability to tune a plasma drive is the ability to experimentally measure and correlate the drive with the initial conditions in the multiple component reservoir. An added bonus would be the ability to accurately predict, through simulation, the results of the plasma gradient piston in order to guide the initial fabrication of the reservoir. The experimental requirements can be divided into two parts: the behavior of solid density material layers and their behavior in a plasma piston drive, and the behavior of various foam density layers. The ability to successfully model the created plasma drives via simulations requires the ability to predict the material response during unloading either analytically (e.g., the formulas shown above) or via the use of tables.

We will address the behavior of several solid and foam layers in a plasma piston drive and show, in some cases, that simulation can be made to match experiment and successfully guide the development of a plasma piston drive. In so doing, we will show that a multiple component reservoir is feasible, tunable, creates a planar drive, and can be simulated. This paper also presents the integration of a solid and multiple foam layers to create a ~3.5 Mbar quasi-isentropic drive.

II. EXPERIMENT

The experimental platform for our study utilized a target package attached to the side of a gold hohlraum. For Omega experiments, the hohlraum dimensions were 7014 μm long by 4000 μm in diameter with a 2400 μm diameter laser entrance hole (LEH) (see Figure 3). A 1 μm Au wall was used to postpone the late-time hohlraum effects8,10 (manifested as an unwanted late-time shock in the velocity profiles) beyond the time window of interest in the measurements. A ~25 μm thick Au cone was used as a stray light

shield and to keep plasma out of the VISAR line-of-sight at late times. A 2000 μm diameter hole on the side of the hohlraum was used to induce an ablation driven shock into the package reservoir mounted concentrically with the side-hole on the outside of the hohlraum. NIF hohlraum dimensions were larger: 13.5 mm in length, 10 mm in diameter, 7 mm diameter LEH, with 5 mm diameter hole on side of hohlraum for a target package.

The target packages consisted of a drive reservoir separated from the drive plate by a silicon or aluminum spacer. The drive reservoir was a stack of materials including an ablator (CH or Be), a reservoir material to absorb high-energy x rays from the hohlraum environment (BrC_4H_3), and other lower density materials such as carbonized resorcinol-formaldehyde (CRF) foams with engineered densities. The thicknesses of the reservoir materials were typically achieved by machining on an ultra-high-precision lathe with a single-crystal diamond tool, with the exception being beryllium, which was mechanically polished to thickness. The reservoir stack was held together by a glue joint around the circumference. The drive plate (~ 10 - 15 μm thick Al or Ta) was backed by a transparent window [LiF and/or *z*-cut quartz (SiO_2)], which also served to tamp the drive. For the NIF targets, LiF and quartz windows were used in a side-by-side configuration, which enables characterization of the drive through the entire pressure range; LiF becomes opaque to the VISAR laser for shocks > ~2 Mbar[11], and the shock front in quartz becomes reflecting for pressures > 2 Mbar.

In order to understand the applied pressure drive profile on the target sample, we utilized the particle velocity (U_p) measured from a witness sample made of Ta or Al backed by a LiF window. We employed a line VISAR (velocity interferometer system for any reflector) diagnostic[11,12] for these U_p measurements. VISAR is an interferometer with unequal path delays that measures the motion of the reflecting surface. Using the recorded particle velocity, along with the known EOS of the witness sample, a back-integration analysis technique will generate the time dependent pressure, $P(t)$, that was applied to the front of face of the sample. For our experiment, we typically used 45 mm and 60 mm etalons that provided 0.854 and 0.641 km/s per fringe once the index of refraction correction for the LiF window was taken into account.

The use of two legs of VISAR with different etalons was to help eliminate the fringe phase ambiguity that occurs when a shock was present. A typical example of VISAR data is shown in Figure 4.

To produce the large shocks needed to make a plasma gradient piston drive we utilized the radiation environment inside of a hohlraum to produce an ablation-driven shock into a package that was mounted on the side of the hohlraum (see Figure 2). Laser beams were pointed such that they did not deposit any significant amount of energy at the opening at each end of the hohlraum with the laser spots forming two rings, one near each laser entrance hole. For the Omega laser facility, 351 nm wavelength lasers delivered 18 – 20 kJ of energy over ~1 ns with a near constant power vs. time profile. Experiments were performed with and without phase plates with no appreciable difference noted in the resulting pressure drives. Experiments performed at the National Ignition Facility (NIF) utilized a ~725 kJ, 2.5 ns FWHM flat-top laser pulse at a wavelength of 351 nm with continuous phase plates. At NIF both a gas-filled and vacuum hohlraum were tested with the best results obtained from a gas-filled hohlraum (~25 Torr at room temperature of C_5H_{12}) that had a 600 ps long foot ahead of the main laser pulse to burn through the polyimide window used to contain the gas in the hohlraum. The Omega experiments utilized vacuum hohlraums.

Peak radiation drive temperatures in an Omega hohlraum were typically 125 – 130 eV and peak NIF temperatures were 192 ±2 eV as determined by the Dante[13] diagnostic. The Dante measured the spectrally and temporally resolved x-ray flux with nominally 15 discrete broad band spectral channels between 50 eV and 10 keV with a temporal resolution of ~150 ps. Each channel consisted of a different set of x-ray filters, mirror and x-ray diode (XRD) that were optimized to measure a particular spectral region. Absolute flux measurements were possible since all components were absolutely calibrated, and the geometry of the system was known. The time resolved spectra, x-ray flux and effective radiation temperature from a given target were determined from the recorded channel voltages by using an unfold algorithm and the photometric response functions of each channel. The unfold algorithm for spectral reconstruction does not inherently have a simple analytic method to quantify uncertainties. Therefore, a

brute force Monte-Carlo (MC) uncertainty analysis[14] was applied which addressed both the uncertainties in the unfold algorithm and the uncertainties in each of the component responses (e.g., filters, XRDs, attenuators, etc.)[15]. The MC analysis generated error bars for the spectra, radiation temperature (T_r) and flux as a function of time.

An equivalent radiation temperature was extracted from 2D hohlraum simulations by integrating the radiation transport equation along a 60 x 60 square grid array of rays passing through the center of the laser entrance hole of the hohlraum and pointed at the angle of observation used by the Dante diagnostic (~37.2 degrees). The integrations were performed for experimental time intervals of approximately 50 – 100 ps. The resulting energy was then assumed to be Planckian in nature and the equivalent radiation temperature was extracted from the simulations to give a T_r vs. time that was then compared to the experimental T_r vs. time values produced by the Dante diagnostic.

III. RESULTS

As noted in the introduction, both solid density materials and low density foams were employed in the reservoir to make a precision pulse shape via a plasma gradient density. We approached the problem of making a plasma gradient piston drive by addressing the behavior of solid density materials first and then integrating them with lower density foams. The results are shown below and are separated into two groups: single component reservoirs and multiple component reservoirs. Single component reservoirs are defined as being reservoirs where only one component of the reservoir was directly measured in the VISAR time history. Multiple component reservoirs are where more than one density layer in the reservoir was measureable in the VISAR time history.

A. Single Component Reservoirs

Single component BrC_4H_3 reservoirs, similar to those used by Smith et al[16] in 2007, were indirectly driven with an initial ablation shock created by a hohlraum wherein ~18-20 kJ of energy was deposited via 3ω (351 nm) laser beams of ~1 ns duration. The reservoirs created ramped pressure drives to peak pressures of ~1 Mbar which are comparable to, albeit lower than, the peak pressures measured by Smith et al or Lorenz et al5 (~ 2 Mbar in driven Al). Pressure drive measurements inferred from VISAR of the Al and/or Ta drive plate tamped with LiF indicate that the energy initially in the ~1 ns long laser beams has produced ramp pressure drives with rise times to peak pressure of the order ~5-8 ns and full-width half-maximum (FWHM) dwell times on the order of 10's of ns (see Figure 4(b)).

Single component reservoirs with SiO_2 in either solid or aerogel form were also measured and analyzed but are addressed separately in Appendix A.

B. Multiple Component Reservoirs

Following the measurement and analysis (see Analysis section below) of BrC_4H_3 single component pressure drives, plasma gradient piston drives were measured for several multiple-component reservoirs: BrC_4H_3 (2 g/cc) + $Br_2C_{50}H_{48}$ (1.2 g/cc); BrC_4H_3 (2 g/cc) + 0.5 g/cc CRF foam; BrC_4H_3 (2 g/cc) + 0.10 g/cc CRF foam; and BrC_4H_3 (2 g/cc) + 0.50 g/cc CRF foam + 0.050 g/cc CRF foam reservoirs.

The multiple component density reservoir of 150 μm BrC_4H_3 (2.0 g/cc) + 50 μm $Br_2C_{50}H_{48}$ (1.2 g/cc) was investigated to test the feasibility of multiple solid-solid reservoir materials at differing densities for high pressure designs. The hohlraum conditions that produced ~1 Mbar drives on ~10 μm Ta samples were used. As seen in Figure 4, the VISAR history clearly shows the arrival and drive created from the 50 μm $Br_2C_{50}H_{48}$ layer and a shock or discontinuity in the velocity after the peak velocity which is not present in the simple ~1 Mbar (BrC_4H_3) velocity profile.

To investigate the use of foam components in creating plasma gradient piston drives for conditions more relevant to the NIF drive shots, two changes were made in the experimental setup to increase the shock strength at the back of the reservoir: the ablator thickness was thinned from 75 μm to 25 μm Be, and the BrC_4H_3 layer was thinned to 50 μm. Velocity measurements of a ~10 μm Ta sample placed behind the BrC_4H_3 layer revealed no measureable movement of the sample during laser deposition in the hohlraum, in agreement with simulations that showed that a 50 μm layer of BrC_4H_3 was more than sufficient to shield the sample from possible radiation-induced heating due to the high-energy x-rays produced in the hohlraum. Additional layer(s) were then added to the base reservoir of 25 μm Be + 50 μm BrC_4H_3 to measure their effect on the plasma gradient piston drive. 100 mg/cc, 500 mg/cc, and 50 + 500 mg/cc CRF foams were investigated and produced measureable plasma gradient piston drives (see Figure 5 for 500 mg/cc and 50 + 500 mg/cc foam results). The package for the double layered foam employed a stepped LiF window which provided simultaneous measurement for two different gap sizes. In all multiple component reservoir cases involving foam, the arrival of the BrC_4H_3 layer caused the LiF window to become opaque to the VISAR diagnostic indicating the shock on the LiF window was > 2 Mbar.

The experimental velocity drive measurements performed at the National Ignition Facility resulted in a stepped velocity vs. time profile (see Figure 6). The peak radiation temperature measured using Dante was ~192 ± 2 eV. Velocity measurements were made through the SiO_2 and the LiF windows. The velocity data shown in Figure 6(b) was measured through the LiF window which stayed transparent past peak velocity.

IV. ANALYSIS

Pressure vs. time information was derived from simulations of a plasma drive that were made to match experimental drive plate velocities as measured by VISAR. We outline the method that was used in fitting the BrC_4H_3 reservoirs below since the process was representative of all the plasma drives measured at the Omega Laser Facility and, to some extent, the drives measured at the NIF as well. The matching of

the simulated drive plate velocity to experimentally measured data was split into two steps: matching of the initial rise time and rise-to-peak velocity, and matching during and after peak velocity was achieved.

The matching of the first part of the BrC_4H_3 drive with simulations required accurate measurement of the rise-time and peak velocity of the VISAR data. Absolute timing between the laser power histories and the VISAR velocity information was obtained via the timing fiducials present on each raw VISAR image. A separate shot was carried out to absolutely calibrate the timing fiducial marks to the laser time. The velocity information from the raw VISAR image was obtained by converting the measured fringe pattern into a phase map, and then converting the phase map to a velocity map using the known sensitivity (i.e., velocity-per-fringe) determined by the chosen etalon thickness and velocity correction for the shocked transparent LiF window[17,18]. 2D simulations of the hohlraum environment were conducted using the as-measured dimensions of the hohlraum, and the laser pointing and laser power vs. time values as provided by the Omega or NIF laser facility. The inherent 3D nature of the side-mounted package with its lower albedo ablator material was included in the 2D simulations as an azimuthally symmetric ring around the middle of the hohlraum. The dimensions of the low albedo ablator were set such that the surface area of the 2D band and the surface area of the side mounted package exposed to the interior of the hohlraum were equal. A frequency dependent source (FDS) was then generated from a group of 36 zones located at approximately 300 μm off-axis at the center of the hohlraum by taking the average of the energy density in each of the 60+ energy bins. The energy density of each bin was summed over the zones at each time step and the average value over the preceding ~105 ps was recorded. Since the experimental line-VISAR data indicated that the plasma gradient piston drive on the drive plate was one-dimensional (i.e., negligible edge effects), one-dimensional simulations driven by the FDS were employed to model the package response to the hohlraum radiation environment. Tabular equation-of-state tables were used for each of the package materials (including the CRF foam). For Omega hohlraum reservoirs an overall multiplier was applied to the energy densities recorded in the FDS that ranged from ~0.72-1.0 (resultant

T_r range was 125-132 eV) until the initial rise-time and rise-to-peak velocity of the drive plate in the simulation matched those measured by VISAR.

For the Omega ~1 Mbar drives, the match of simulation to experiment at and after peak velocity was not as straight forward and required the manipulation of the density and the velocity profiles in the unloading reservoir just prior to the reservoir's initial impact on the drive plate. As a check on the methodology of the simulations, simulations of the previous ~2 Mbar drive which utilized a BrC_4H_3 single component reservoir used in the experiment by Smith et al16 were carried out and matched to within the velocity error bars of the ramp drive during the entirety of the measured ramp drive (see Figure 7). A match was done self-consistently in the hydrodynamics code with the tabular EOS tables and did not require the manipulations of the density or velocity profiles. In an attempt to understand why the lower drive required manipulation of the density and velocity profiles to match data, a comparison of the simulated density and temperature paths of the BrC_4H_3 between the ~2 Mbar drive and current ~1 Mbar drive was done. The comparison revealed that the strength of the shock at the back of the BrC_4H_3 reservoir was very different (~8 Mbar vs. ~2.5 Mbar) and that even though the density range was about the same during release the minimum release temperature was lower in the lesser drive case (~1 eV compared to ~2 eV). An investigation of the simulations revealed that the rise-time and the peak velocity of the drive were set by the integration of the radiation temperature in the hohlraum to a few nanoseconds after peak radiation temperature. We tried to adjust the simulated post-peak drive velocity by adjusting the time history of the radiation drive after peak temperature but found that we could not simultaneously match the rise-time and rise-to-peak drive velocity produced by the drive as well as peak and late-time velocity profile. We concluded that a self-consistent simulation from the simulated hohlraum drive and the initial conditions of the reservoir utilizing our present tabular EOS table for BrC_4H_3 could not produce a precise match to the measured velocity at late-times for the ~1 Mbar pressure drive (see Appendix B for further discussion) and created a plasma drive8,[19] (as explained below) to reproduce the drive.

To match the simulations with the data for the weak shock case, we recognized that the velocity vs. time profile measured by VISAR was primarily dependent upon the ram pressure ($\rho(x)u(x)^2$) of the incoming plasma drive with only a weak dependence upon temperature and that the measured velocity vs. time curve could be reproduced in the simulation by changing the spatial velocity and density profiles of the incoming plasma gradient piston. We recognize that any solution found that reproduced the measured velocity profile would not be unique but would be a way of producing a simulated drive from which we could extract drive pressure information. We chose, as initial conditions for the plasma gradient piston drive, the density, temperature, and velocity profiles of a simulation that matched the initial rise time and rise-to-peak velocity of the experiment at the time just prior to interaction between the reservoir material and the front of the drive plate. We assumed that the EOS of the Ta drive plate and LiF tamper to be correct under compression and then adjusted the velocity and density profiles of the upstream zones responsible for producing the drive at and after peak velocity to reproduce the measured velocity vs. time profile at the back of the drive plate. Once the simulated and experimental velocity vs. time curves matched, the pressure vs. time history of the plasma gradient piston at the front of the drive plate was extracted from the simulation.

Multiple component reservoirs were investigated using BrC_4H_3 as a density layer and as the blocker of hard radiation (>1 keV) from the hohlraum environment. A solid/solid reservoir material was used to test the measurement capability of being able to correlate parts of the drive back to the initial density profile in the reservoir. As shown in Figure 4(b) above, the arrival of the interface between the two reservoir materials is clearly seen and agrees with the timing of a simulation that uses the same peak radiation temperature (127 eV) as was measured with the Dante diagnostic. The lack of agreement in velocity between the simulation and the data was also seen in single component reservoirs and corresponds to the simulations using unconstrained parts of an EOS table (see below and Appendix B). Correlation between the measured drive and the initial reservoir materials was also measured for several CRF foams at different initial densities: 100, 500, and 50+500 mg/cc. In all cases interfaces between the individual

density layers in the initial reservoir produced measurable jumps in the VISAR velocity history. This means that the measurement of the interface positions in the VISAR drive history and knowledge of the initial density profile can be used to tailor individual parts of the pressure vs. time history to produce a desired pressure vs. time history.

The data from single and multiple component reservoirs utilizing CRF foam on Omega had to have a multiplier applied to the FDS source to match the rise time and the peak velocity. Drive data from a single shot of multiple foam layers (50 + 500 mg/cc CRF foam) simultaneously crossing 300 and 500 μm gaps were used to try and simulate the evolution of the CRF foam as it crossed the gap. Simulations of the multiple foam layers on Omega could be made to match either the 300 or 500 μm gap but not both with a reduction of 15% in the FDS drive source. The inability to match both gaps with the same drive indicated the simulations were not capturing all of the relevant physics and raised the possibility that the tabular EOS used for the CRF resulted in a good approximation of its behavior but was not entirely accurate. The arrival time of BrC_4H_3 interface was also not in agreement with simulation with a slightly thicker (~10% thicker) foam layer required to match the interface arrival as seen in the data. Only the timing of the shock created by BrC_4H_3 arrival could be used to calibrate simulations since the LiF blanked upon BrC_4H_3 impact for all of the Omega CRF shots. In the Omega experiments, both single and double layers of CRF foam behaved in rough agreement with simulation but post-shot simulations with multipliers were required to match the data within the experimental error bars.

Drive data for NIF CRF foam did not require a thickness multiplier or a time shift in the simulations to match the rise time but did require an increase in the initial density of the foam. Since the strength of the shock in the CRF foam was stronger than in the Omega data, the discrepancy between the simulation and the data was expected to be less – similar to what was observed in the BrC_4H_3 data. A comparison between pre-shot simulations and data showed good temporal agreement between features in the drive but poor agreement in the resulting velocity for each CRF step with the disagreement being proportional to the CRF foam density. In the simulations the 50 mg/cc was raised to 62 mg/cc and the 500 mg/cc was

raised to 800 mg/cc in order to match the peak velocity and rise time behavior of the drive corresponding to the CRF foam steps (see Figure 6). The mix model parameters used to match the Omega foam step data were also used in the NIF simulations. Simulated shock strength at break out from the BrC_4H_3 was ~12 Mbar and, in agreement with the simulations of the ~8 Mbar shock break out data, a self-consistent simulation using the FDS source and the initial reservoir conditions was used to fit the part of the drive data corresponding to the BrC_4H_3. The fit of the drive corresponding to the BrC_4H_3 was used to constraint the FDS energy multiplier used (1.01 for these simulations) when fitting the CRF foam data. The lack of shocks in the velocity data indicated that the pressure drive was quasi-isentropic throughout the ~14 μm Ta sample. Pressure drive information taken from the matched simulations indicated that a peak pressure of ~3.5 Mbar was achieved 2μm from the front of the ~14 μm Ta sample. A comparison between the pre-shot simulations and the measured data appears to confirm showed that even though the EOS used for the CRF foam was not accurate during release for the densities used that the drive timing and peak velocity (pressure) were in good agreement. Such agreement indicates that the simulations are a useful tool for the design of the reservoir for this CRF/BrC_4H_3 drive system but an exact match to the measured drive requires the use of post-shot simulations with density multipliers.

Repeatability of the hohlraum drive conditions at the Omega Laser Facility was a concern since the data was taken over a period of years and, of necessity, spanned multiple shot days during that time period. Several diagnostics (Dante, laser power history, total laser energy into the hohlraum) were investigated to try and determine the repeatability of the hohlraum ablation conditions and the resulting plasma drive. The best correlation was with total laser energy into the hohlraum (energy varied ~10% while the peak drive velocity varied ~15%). Simulations of the radiation temperature using the as-shot laser power profiles and the as-built target metrology values yielded T_r values between ~128 and 136 eV. We found the T_r as determined by Dante was not always a good indicator of drive conditions for comparing hohlraums shot on different calendar days but was reliable when used to compare drives measured on the same shot day. Our lack of correlation between radiation temperature as determined by Dante and the

drive velocity (which has a close to linear correlation with pressure at our peak velocities) can be seen most readily by comparing the ranges of their values. Radiation temperature was found to vary from 110 – 133 eV for nominally the same amount of laser energy (18 – 20 kJ) entering the hohlraum with no evidence of beam clipping at the laser entrance hole. The resulting plasma gradient piston drive as measured by VISAR was found to vary (peak velocity varied by approximately ±15%) from shot day to shot day for the same type of reservoir but was quite consistent during the shot day (see Figure 8 for measured scatter in T_r). Target variation due to different target builds was ruled out by experimental Dante and VISAR measurements of different builds of targets measured on the same shot day resulting in the same plasma gradient piston drive results and the same measured Dante T_r (within the error bars). To gauge the expected difference in drive velocities due to measured Dante T_r variance, we used the scaling given by Lindl[20] which gives the ablation pressure as being $\sim Tr^{3.5}$ which means that if the determined Dante values were correct the range in the measured peak drive would vary by a factor $(133/110)^{3.5} \sim 2$ which is much larger than the ±15% factor observed in the data.

In an attempt to quantify edge effects on the uniformity of the plasma drive we analyzed the spatial drive uniformity measured by the VISAR diagnostic. Experimental VISAR data indicated that the plasma gradient piston drive at the drive plate in the region of interest was spatially planar to within 150 ps. Application of the "45° rule" which states that the edge effects for a planar drive have a geometrical event horizon that is at most 45° from the point at which the drive is non-planar, indicated that a non-uniformity in the spatial extent of the drive would have been evidenced in the Omega data. For the Omega hohlraums the largest the distance between the front of the ablator and the back of the drive plate, $d_{Standoff}$, was ~650 μm. The application of the "45 ° rule" implied that the originally ~2 mm planar drive region at the front of the ablator would be reduced to ~700 μm at the back of the drive plate. The observed line-VISAR fringe-pattern used at Omega (see Figure 4(a)) was centered on the middle of the drive plate and had a spatial extent of > 1100 μm. Negligible spatial or time variation was observed between the edge and the middle of the measured region indicating that the actual geometrical degradation of the planar

drive due to edge effects for this platform is < 35°. The angle of disturbance for the NIF platform ($d_{Standoff}$ = 1500 μm, VISAR FOV = 2 mm) following similar arguments can only be constrained to be < 45°. In both cases a uniform drive in space and time (<150 ps) was produced at the back of the drive plate.

V. CONCLUSIONS

We have investigated plasma gradient piston drives created from both single and multiple component reservoirs. We have shown that BrC_4H_3 single component reservoir drives match simulations for strong shocks (≥8 Mbar at shock break out) in the reservoir and that plasma drives can be used to match shocks producing lower drives (~2.5 Mbar at shock break out). Pre-shot simulations are shown to be in rough agreement with measured drive data but post-shot simulations with density and velocity multipliers are required to give an exact match for the ~1 Mbar drive data. SiO_2 release data is not in agreement with simulations indicating that the simulation code and the release portion of the EOS table do not accurately represent the measured drive of the releasing material. Work presented indicated that the discrepancy is due to a phase change in the SiO_2 during release (see Appendix A).

The inclusion of multiple density components (whether solid or foam) into the reservoir were shown to increase the ability to tune the pressure drive on a sample. Each density layer at the length scales used has been shown to create a distinct signature in the velocity history profile that can be directly correlated with the initial spatial density profile of the reservoir. The ability to correlate individual drive features to the initial reservoir conditions allows for the tuning of the drive by changing the initial conditions of the multiple component reservoir.

We have also shown that the combination of solid and foam layers created a ~3.5 Mbar quasi-isentropic drive at the Nation Ignition Facility and that simulations were a useful tool in predicting the drive profile. Post-shot simulations were made to match the measured drive; conditions for the match (500/50 mg/cc CRF steps changed to 800/62 mg/cc CRF) indicated that the EOS used for the CRF foam was not

accurate during release but that a change in the simulated densities was sufficient to bring the simulated drive and the experimental drive into agreement.

A measured ~1 Mbar drive has been shown to be repeatable at the Omega Laser Facility over a period of over two years. Drive shots on different days are correlated with the total laser energy into the hohlraum and not the Dante determined T_r albeit that Dante determined T_r is a good relative measurement for drive shots done on the same day.

Drive uniformity has been shown to be uniform with a temporal variance < 150 ps. Edge effects have not been measured in the line-VISAR placing a limit on the geometrical extent of drive uniformity degradation due to edge effects of being < 35° from target surface normal for the Omega experimental platform.

In closing, we have shown that the initial concept of the plasma drive piston as demonstrated by Barnes et al with high explosives has been successfully demonstrated with laser-driven systems where a strong shock is used to create an unloading plasma that, upon stagnation, creates a plasma piston drive. There is no constraining physics that limit the use of the tailored pressure drive to a laser-driven system. The physics can be applied on any facility that can produce a large enough (multi-Mbar) planar shock. Thus, the ability to investigate off-Hugioniot states by the use of tailored pressure drives is only limited by the lateral extent and strength of shock that a facility can produce.

Acknowledgements

This work performed under the auspices of the U.S. Department of Energy by Lawrence Livermore National Laboratory under Contract DE-AC52-07NA27344. LLNL-JRNL-520653

Appendix A

Pre-shot simulations indicated that the predicted material response of solid SiO_2 (2.5 g/cc) under our experimental conditions would produce ramped pressure drives with rise times comparable to those of BrC_4H_3 (2.0 g/cc) and SiO_2 aerogel foam would be comparable to carbonized resourcinol formaldehyde foam but with higher peak pressures due to the higher density of the SiO_2. The produced ramp drive of both SiO_2 z-cut quartz and SiO_2 aerogel foam were measured. Further investigation of the compression behavior of SiO_2 aerogel via shock transit time through steps of known thickness were carried out as well as measuring the post-shock release-ramp drive induced on a Al/LiF drive plate. The shock break-out times from the back of the SiO_2 aerogel were in good agreement with simulation. Simulations of the release experiments were also performed but were not in agreement with the experimental arrival times being much later (up to 5 ns in some cases see Figure 9). Peak ramp velocities were in agreement but there was a disagreement in rise times between simulation and experiment.

The large departure of the SiO_2 velocity data from simulation is believed to be due to the inability of the simulations to account for the dynamic material properties of the SiO_2 during its release phase. The Cheetah code[21] at Lawrence Livermore National Laboratory was used to calculate the SiO_2 liquid mass fraction along the release adiabat of SiO_2 as a function of density. Chemical equilibrium was assumed between all species considered: SiO, Si, Si_2, SiO_2, Si_3, O, O_2, O_3, Si^+, Si^-, O^+, O^-, O_2^+, O_2^-, and a free electron. For the densities given in the simulations for the leading edge and rise of the release wave (<1 g/cc) there is expected to be ~50% of the SiO_2 in liquid form (see Figure 10). The presence of the liquid invalidates the assumption made in the introduction of complete vaporization of the reservoir material during shock unloading (i.e., constant γ) and would imply that the internal energy from the shock that would normally create the pressure to drive the expansion of the releasing material is on the order of the interaction energy between the SiO_2 molecules. Under such conditions the ram pressure created by such a releasing reservoir would necessarily deviate from that of a plasma gradient piston since the pressure loss due to liquid formation during the release of the SiO_2 is not taken into account in the assumptions of the

plasma gradient piston or in the radiation hydrodynamics codes used to simulate the experiments. The large departure of the expected SiO_2 (solid or aerogel) plasma gradient piston from simulation indicated an inability to accurately predict drives relying upon the release of SiO_2 for our drive pressures (~3 Mbar at shock breakout) and further experimental effort was redirected into the investigation of CRF foams.

Appendix B

The departure of the drive data from that predicted from the equation-of-state (EOS) table is not surprising if one considers how the EOS table was made and the normal assumptions made in radiation hydrodynamics simulations. For the EOS tables used in the simulations shown here the method outlined by Young et al[22] was followed. Existing data was used to constrain the table for values around the shock Hugoniot and, for some materials, some off-Hugoniot compression data was available and included. A model for material behavior is then assumed and used to extrapolate and interpolate EOS table values. For the tables used, the modeled material response under compression is treated differently from its release behavior when the density drops below it nominal density[22]. No reliable data exists for the material response during release for BrC_4H_3 and CRF foam so the parameters used in the soft-sphere function to adjust the cold curve response of the material for $\rho < \rho_o$ was calculated to give $\gamma_{adiabatic} \cong {}^{6}/_{5}$ and then extrapolated to higher density and temperature values expected for an ionized plasma. Simulations of such a material that relied upon a path through the EOS that traversed the release portion of the EOS table would then become subject to the chosen functional form. If the functional form chosen was wrong or did not capture changes in the internal kinetic energy of the material due to phase changes during release, the deviation between simulation and experiment would be dependent upon the amount of time spent transiting the incorrect release region of the EOS table. In our simulations, we find that the BrC_4H_3 region of the EOS table sampled by the reservoir materials during the low density part of the release wave produces a velocity drive that is in good agreement with experiment. The portions of the reservoir that spend a large amount of gap transit time in the parameter space where the density is relatively high (50 – 400% of solid density) and the temperature is relatively cool (< ~2.2 eV) in the

simulations correspond to where the simulated drive differs from the experimental drive. The inability of the radiation-hydrodynamics code to calculate energy loss due to possibly unknown phase transitions coupled with the lack of data to constrained the functional form used in the release portion of the EOS table are believed to be the primary sources causing the simulation to disagree with the experimental drive for late-time values.

Figure 1

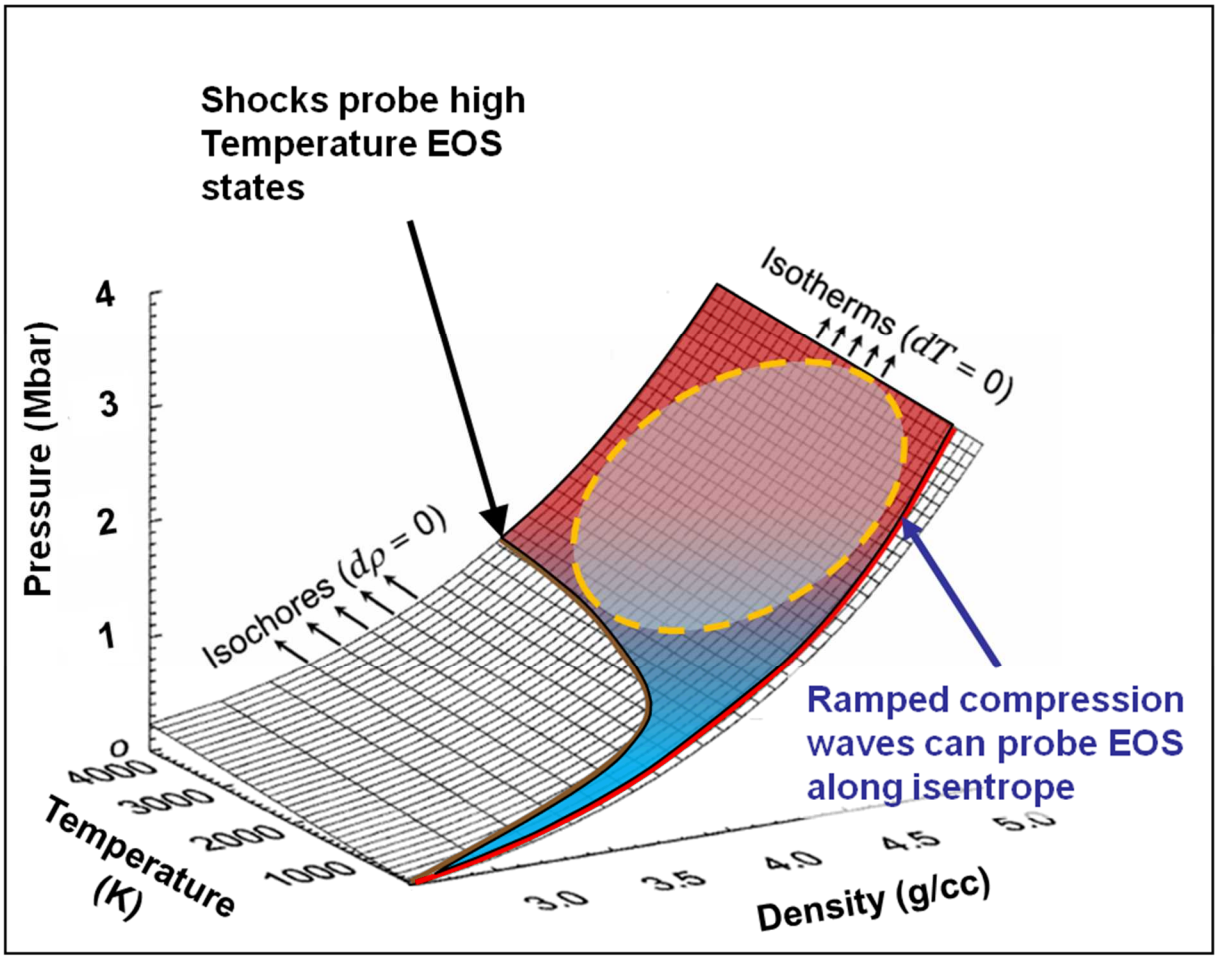

Figure 1 Parameter space for EOS table. Single shock experiments have been used to probe high temperature regions of the table but are limited to the density they can achieve. Compression along the isentrope is not achievable for high pressures (> ~2 Mbar) due to lack of experimental ability to apply such high pressure for an extended period of time. The region of interest for many fields of study is in the circle region between isentropic compression and the shock Hugoniot.

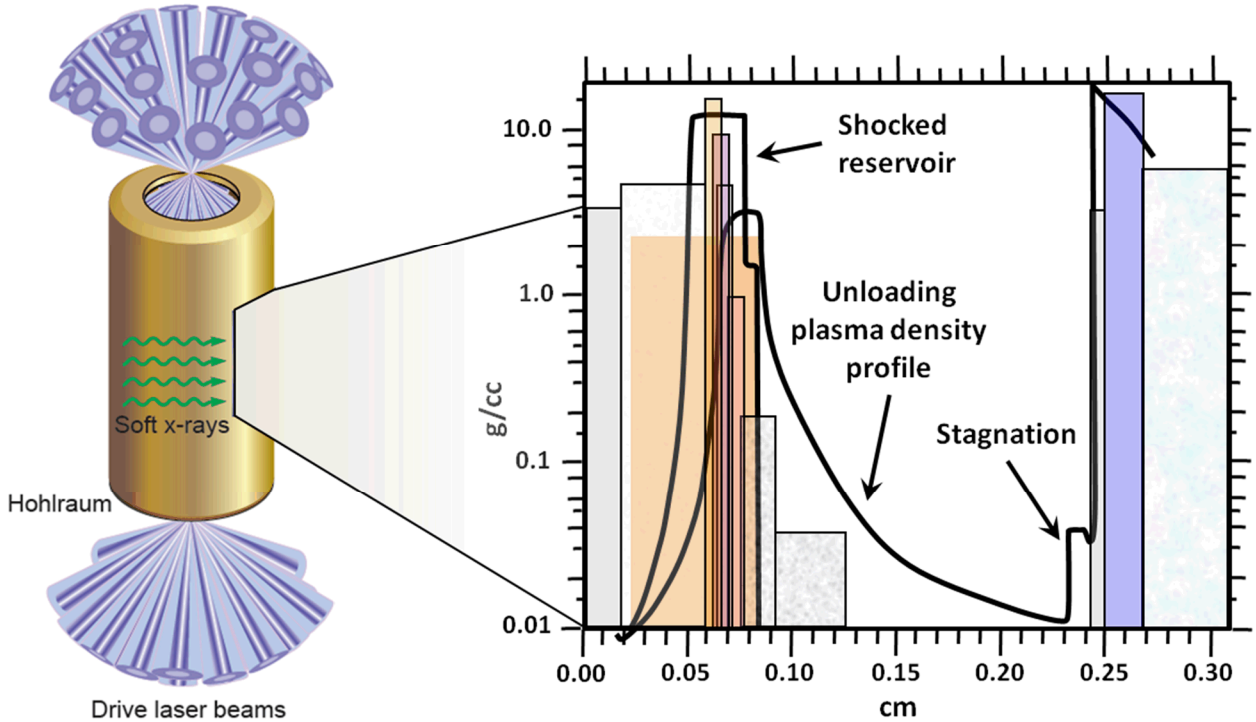

Figure 2 The laser-driven hohlraum on the left drives a shock into the side-mounted reservoir materials which have been expanded to show the initial density vs. position. An overlay of single component reservoir undergoing shock loading, shock release, and stagnation is shown as a bold line to emphasize the evolution of the single component density profile as it crosses the gap and stagnates against the sample. The multiple component drive profile at time=0, shown as stepped density layers, is chosen to approximate that of the unloading, single component profile.

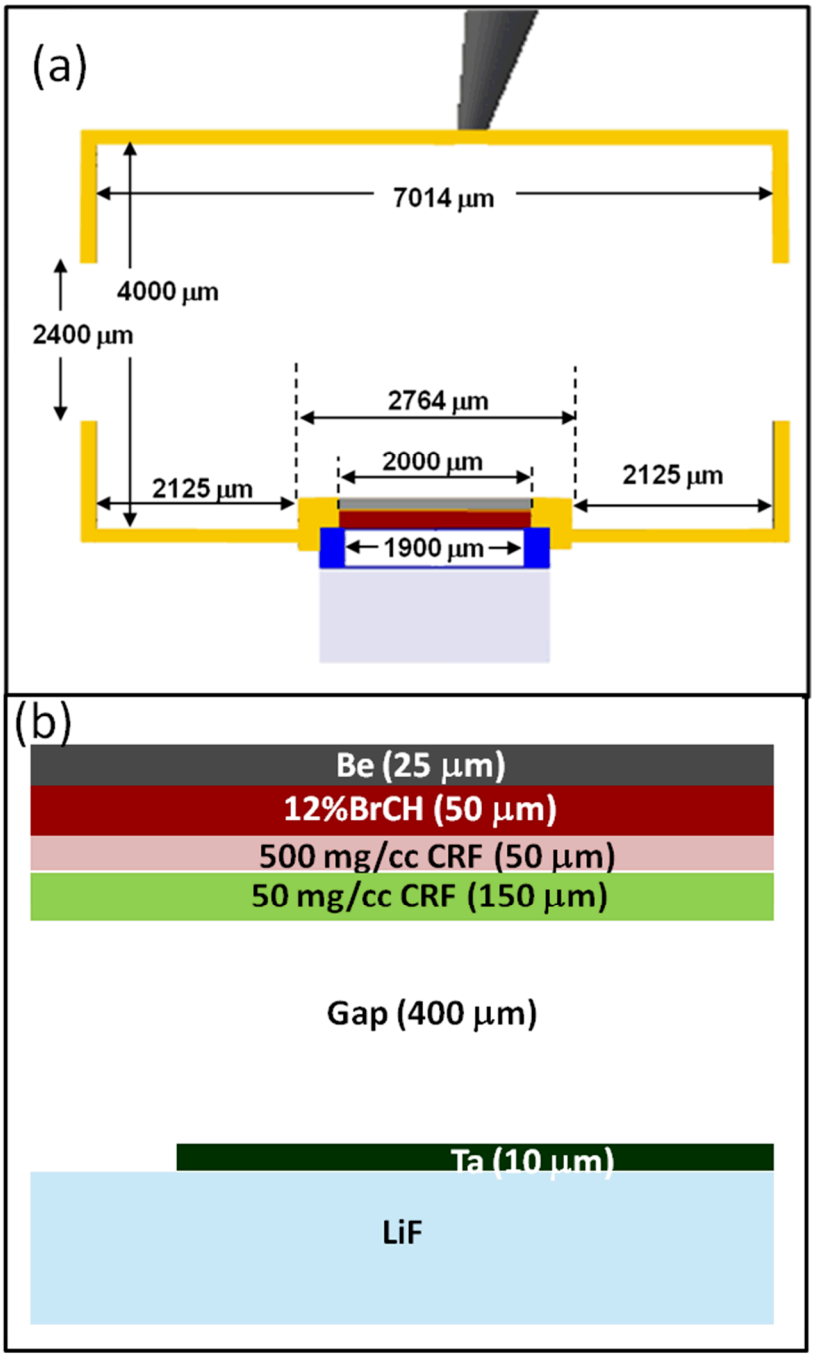

Figure 3 (a) Omega hohlraum dimensions. Hohlraum wall is actually ~1 µm Au backed by ~100 µm epoxy. Laser spots form two rings with each ring located between the side-mounted package and the laser entrance hole. (b) Cartoon representation of side-mounted package in more detail. Shown is the 3 component reservoir where BrC_4H_3 acts as the high-energy x-ray absorber and the layer responsible for peak pressure. The gap in the Ta is a diagnostic hole to allow shock break-out and gap crossing time of the reservoir.

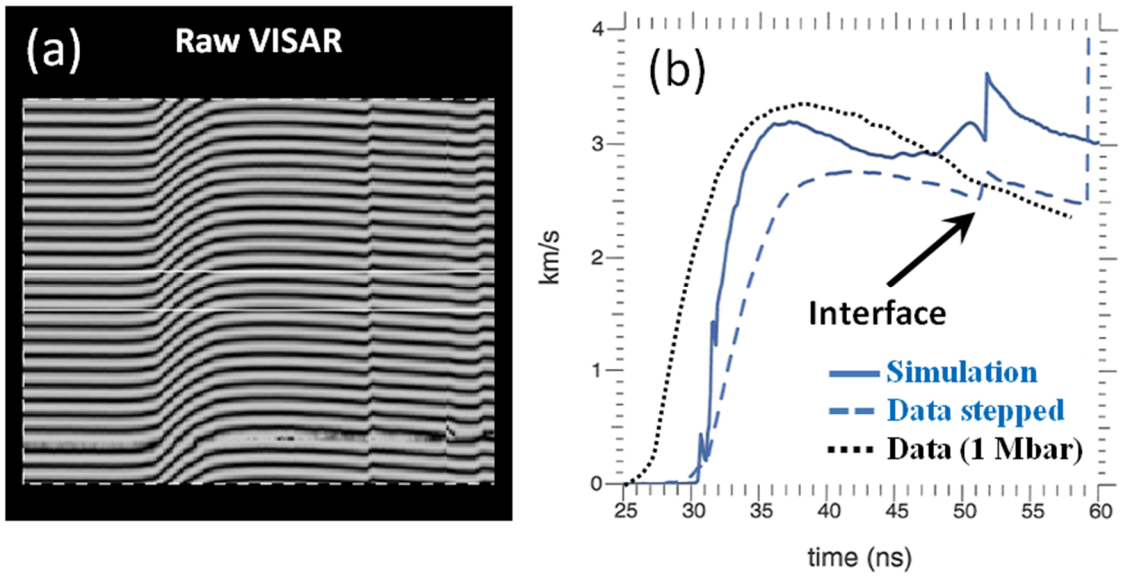

Figure 4 (a) Raw VISAR data showing ramped nature from a 150 µm BrC_4H_3 (2 g/cc) + 50 µm $Br_2C_{50}H_{48}$ (1.2 g/cc) reservoir. Spatial extent is ~1100 µm. (b)Analyzed VISAR data with the shocks resolved into velocity discontinuities. Stepped density simulation is shown for comparison as is the data from a comparably driven, single component BrC_4H_3 reservoir. Shock at ~52 ns labeled "interface" is due to the material interface between the 2 g/cc BrC_4H_3 and 1.2 g/cc $Br_2C_{50}H_{48}$ in the two component reservoir.

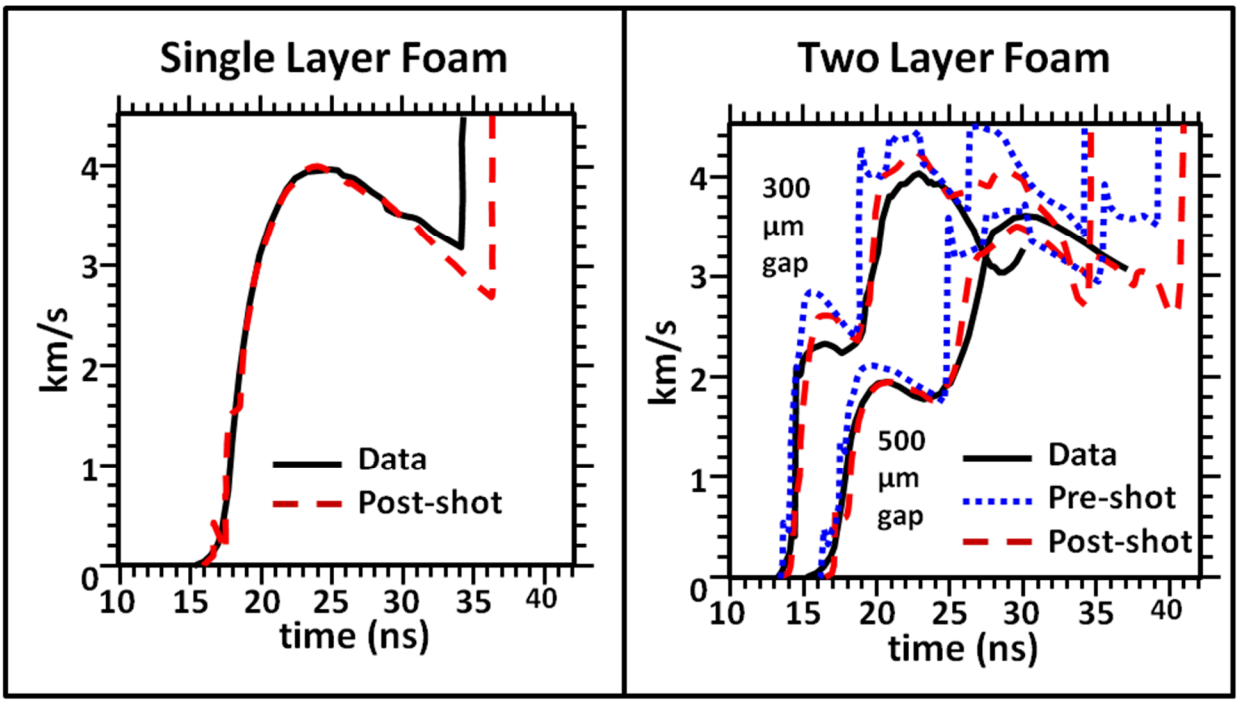

Figure 5 Single and two layer foam results. The single layer 500 mg/cc CRF foam (left) produces a smooth drive profile that has been matched with a post-shot simulation. (Right) The two layer foam steps (500 mg/cc + 50 mg/cc CRF) also produce a smooth, stepped drive profile that has been matched with simulations. The pre-shot simulations shown had the FDS adjusted in order to match the peak velocity in the experimental results. A mix model was used to smooth the transition between the foam layers to obtain the post-shot fit to data. Note that the peak velocities do not match for both gap sizes indicating that the simulation is not capturing all of the relevant physics present in the system.

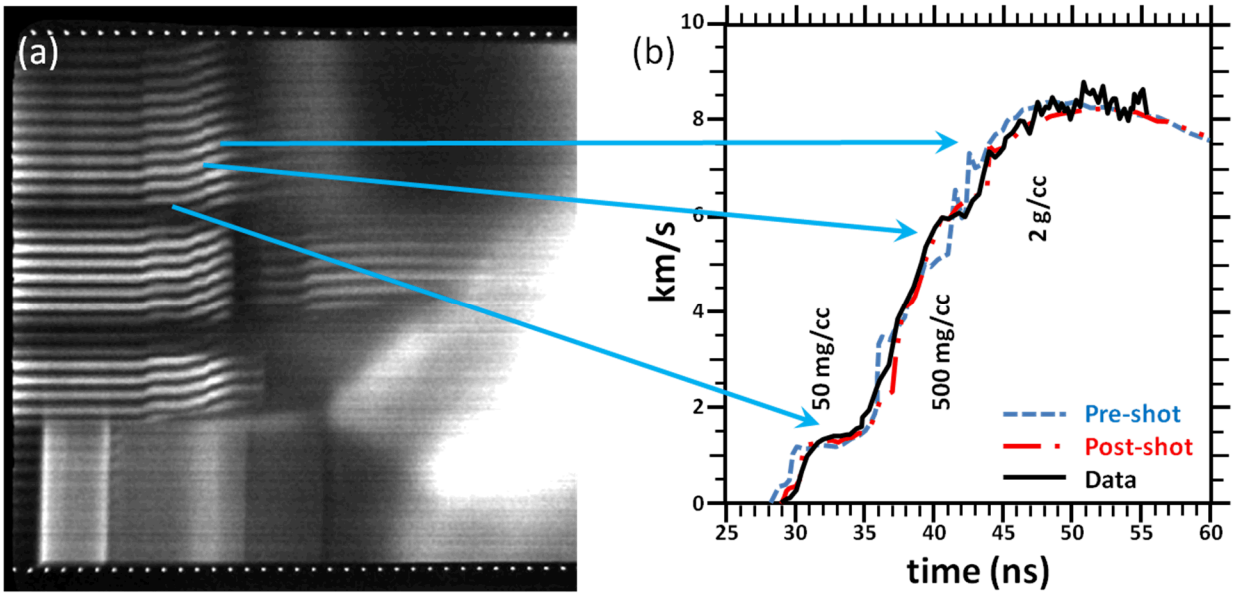

Figure 6 VISAR from a three density layer reservoir gas-filled hohlraum shot from the NIF. The raw VISAR image shows the ramped nature of the drive. The part of the plasma gradient piston drive which corresponds to each layer of the initial reservoir is clearly distinguishable and labeled in the plot on the right. Temporal agreement between pre-shot simulation

and data but post-shot simulation with increased CRF densities (62/800 mg/cc) needed to achieve time and velocity match. All simulations used the same mix-model parameters that were used to fit the Omega results.

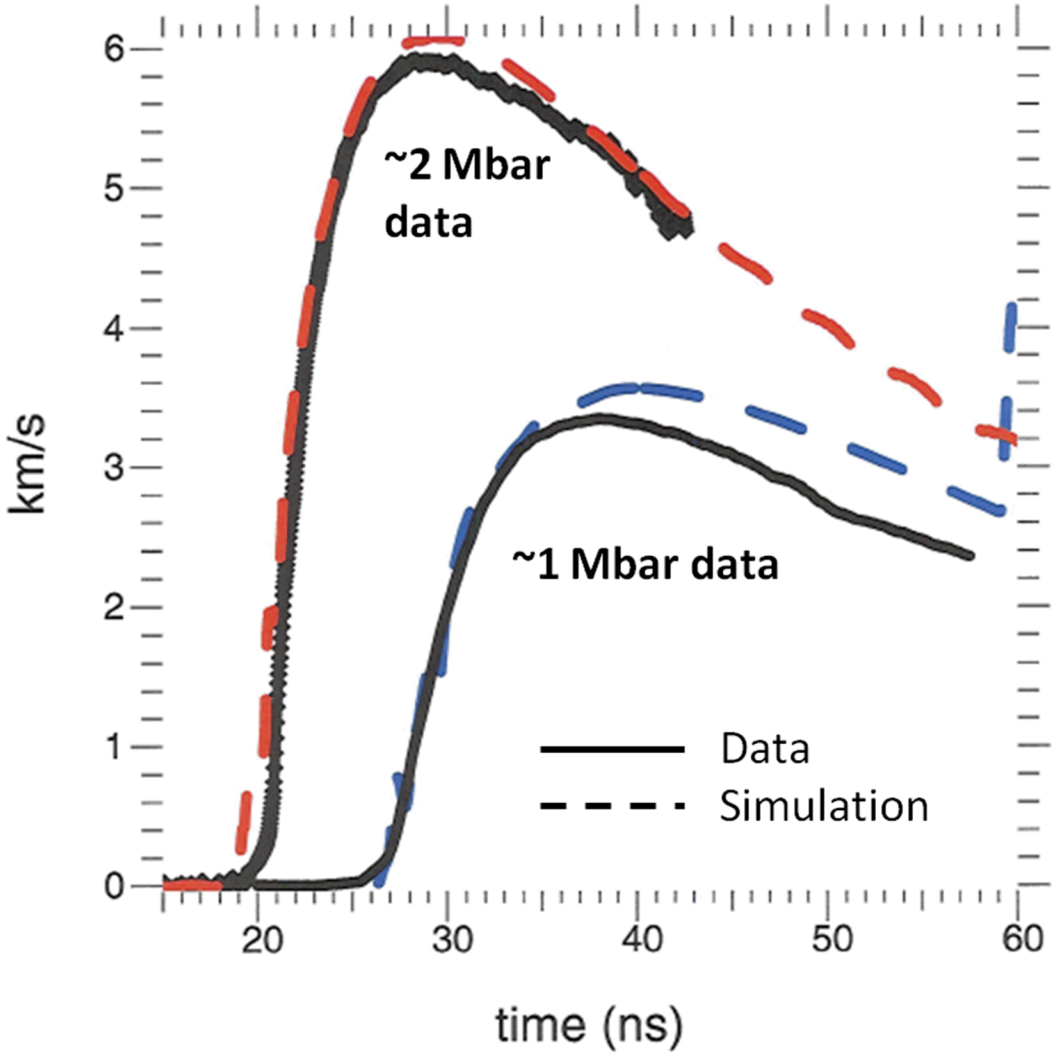

Figure 7 A comparison between measured drive data and self-consistent simulations which utilized the initial conditions of the reservoirs and an FDS source scaled with a multiplier. Simulations of the system with the stronger shock (~8 Mbar at shock break out) are in good agreement with the data whereas the weaker shock system can only be made to match the rise time and rise-to-peak profile.

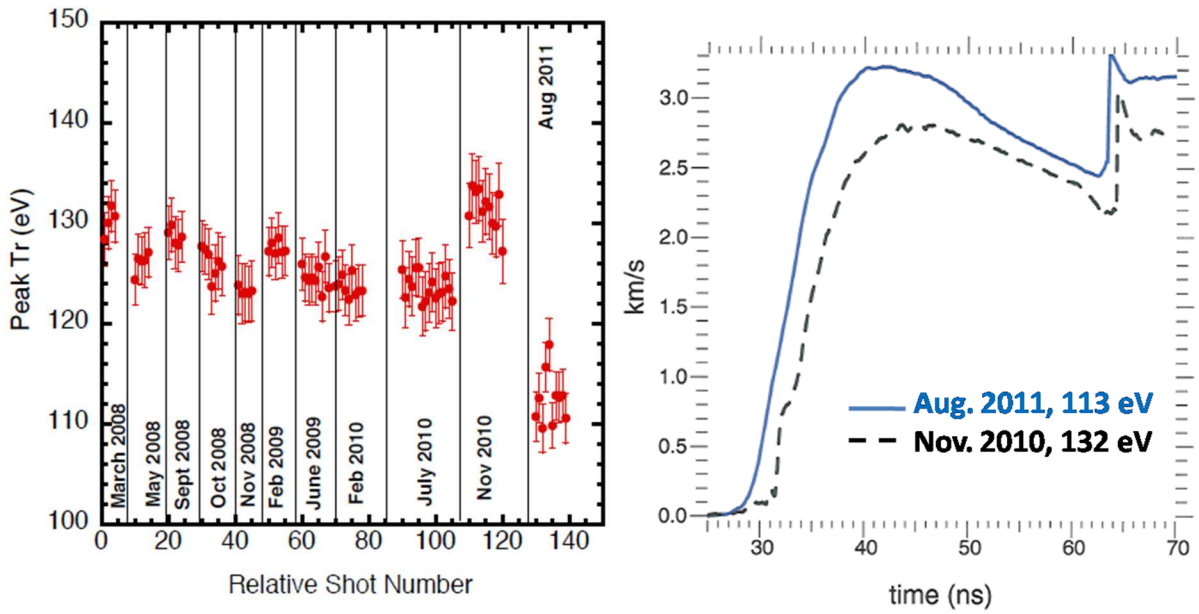

Figure 8 (a) Time history of radiation temperatures as determined by the Dante diagnostic on Omega hohlraums. Dimensions and materials of hohlraums were constant with 18-20 kJ of energy being delivered for each shot day. Calendar time was > 3 years. (b) Measured VISAR drive for two different shot days. Expected pressure scaling is $(113/132)^{3.5}$ ~1.7 but drive peak drive is 3.0 ± 0.3 km/s.

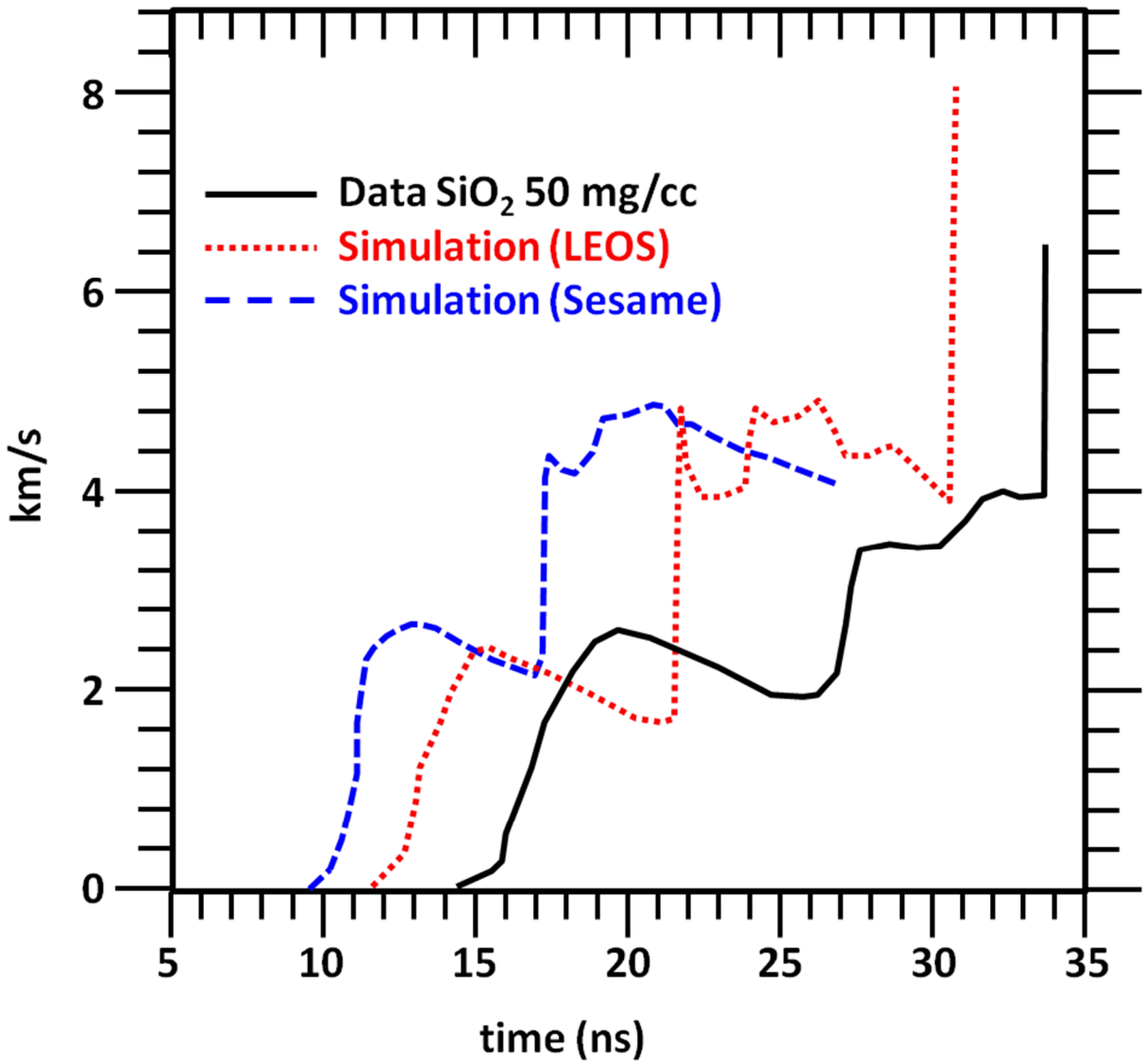

Figure 9 A comparison between meseared SiO_2 aerogel foam drive data (50 mg/cc) and simulation. Results from two different EOS tables are shown. As seen in the graph, the magnitudes of the drives are in agreement but the timing of the drives varies by up to 5 ns for this system.

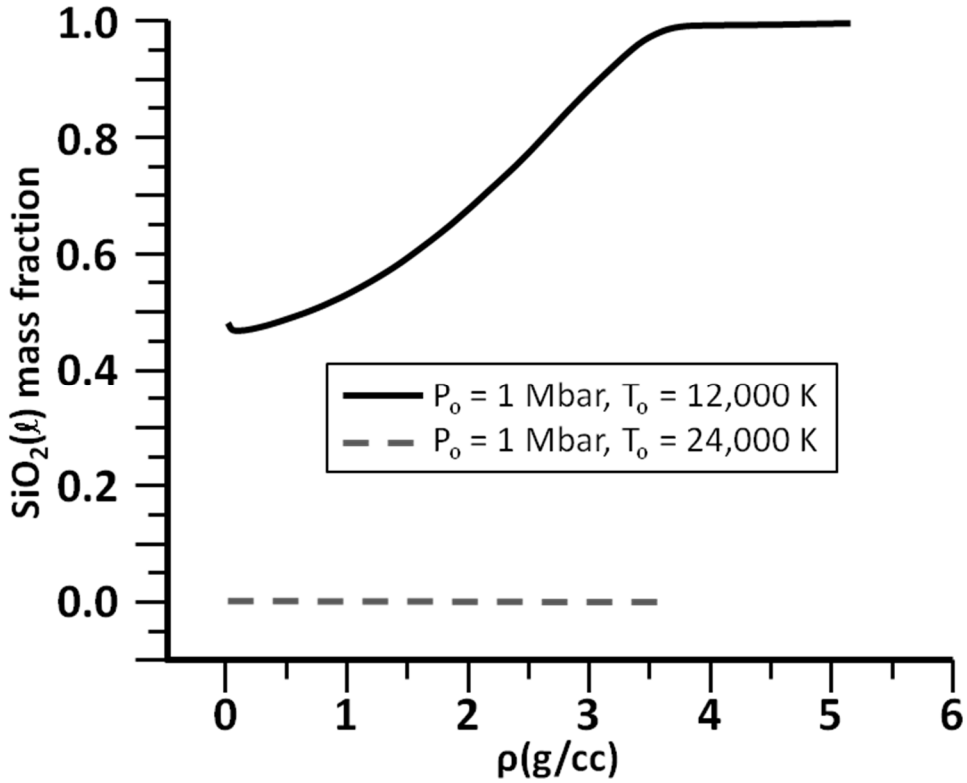

Figure 10 Formation of liquid SiO_2 along the release adiabats for initial conditions of 1 Mbar and 12,000 K and 24,000 K. The simulated densities for the releasing SiO_2 in the single component reservoirs is < 1 g/cc and ~10,000 K which implies that more than half of the releasing SiO_2 material is in liquid form and violates the assumption that the shock causing the release of the SiO_2 is sufficiently strong as to induce complete vaporization (courtesy of Larry Fried and Sorin Bastea).

[1] S. W. Haan, P. A. Amendt, D. A. Callahan, T. R. Dittrich, M. J. Edwards, B. A. Hammel, D. D. Ho, O. S. Jones, J. D. Lindl, M. M. Marinak, D. H. Munro, S. M. Pollaine, J. D. Salmonson, B. K. Spears, L. J. Suter, "Update on Specifications for NIF Ignition Targets," Fusion Science and Technology **51**, no. 4, pp. 509-13 (2007).
[2] G. A. Graham, N. McBride, A. T. Kearsley, G. Drolshagen, S. F. Green, J. A. M. McDonnell, M. M. Grady, I. P. Wright, "The chemistry of micrometeoroid and space debris remnants captured on hubble space telescope solar cells," , Int. J. of Impact Eng. **26**, pp. 263-74 (2001).
[3] John F. Barnes, Patrick J. Blewett, Robert G. McQueen, Kenneth A. Meyer, Douglas Venable, "Taylor instability in solids," JAP **45**, no. 2, pp. 727-32 (1974).
[4] J. Edwards, K. T. Lorenz, B. A. Remington, S. Pollaine, J. Colvin, D. Braun, B. F. Lasinski, D. Reisman, J. M. McNaney, J. A. Greenough, R. Wallace, H. Louis, D. Kalantar, "Laser-Driven Plasma Loader for Shockless Compression and Acceleration of Samples in the Solid State," PRL **92**, no. 7, 075002 (2004).
[5] K. T. Lorenz, M. J. Edwards, A. F. Jankowski, S. M. Pollaine, R. F. Smith, B. A. Remington, "High pressure, quasi-isentropic compression experiments on the Omega laser," High Energy Density Physics **2**, pp. 113-125 (2006).
[6] Hye-Sook Park, K. T. Lorenz, R. M. Cavallo, S. M. Pollaine, S. T. Prisbrey, R. E. Rudd, R. C. Becker, J. V. Bernier, B. A. Remington, "Viscous Rayleigh-Taylor Instability Experiments at High Pressure and Strain Rate," PRL **104**, 135504 (2010).
[7] Hye-Sook Park, B. A. Remington, R. C. Becker, J. V. Bernier, R. M. Cavallo, K. T. Lorenz, S. M. Pollaine, S. T. Prisbrey, R. E. Rudd, N. R. Barton, "Strong stabilization of the Rayleigh-Taylor instability by material strength at megabar pressures," PoP **17**, 056314 (2010).
[8] S. M. Pollaine, B. A. Remington, H.-S. Park, S. T. Prisbrey, R. M. Cavallo, "Design for solid-state Rayleigh-Taylor experiments in tantalum at Omega," Journal of Physics: Conference Series **244**, 042016 (2010).
[9] Ya. B. Zel'dovich and Yu. P. Raizer, *Physcis of Shock Waves and High-Temperature Hydrodymanic Phenomena*, Dover, pp. 37-38 (1996).
[10] O. A. Hurricane, S. G. Glendinning, B. A. Remington, "Late-time hohlraum pressure dynamics in supernova remnant experiments", PoP **8**, no. 6 pp. 2609-12 (2001).
[11] R. Barker and J.. Hollenbach. Appl. Phys. **43**, 4669 (1972).
[12] P. M. Celliers, D. K. Bradley, G. W. Collins, D. G. Hicks, T. R. Boehly, and W. J. Armstrong, "Line-imaging velocimeter for shock diagnostics at the OMEGA laser facility," Rev. Sci. Instrum. **75**, no. 11, pp. 4916-29 (2004).
[13] H. N. Komblum, R. L. Kauffman, J. A. Smith, "Measurement of 0.1-3 keV x-rays from laser plasmas," Rev. Sci. Instrum. **57**, pp. 2179-81 (1986).
[14] M. J. May, K. Widmann, C. Sorce, H.-S. Park, M. Schneider, "Uncertainty analysis technique for OMEGA Dante measurements," Review of Scientific Instruments **81**, 10E505 (2010).
[15] K. M. Campbell, F. A. Weber, E. L. Dewald, S. H. Glenzer, O. L. Landen, R. E. Turner, P. A. Waide, "Omega soft x-ray power diagnostic component calibration at the National Synchrotron Light Source," Review of Scientific Instruments **75**, 3768 (2004).
[16] Raymond F. Smith, Stephen M. Pollaine, Stephen J. Moon, K. Thomas Lorenze, Peter M. Celliers, Jon H. Eggert, Hye-Sook Park, Gilbert W. Collins, "High planarity x-ray drive for ultrafast shockless-compression experiments," PoP **14**, 057105 (2007).
[17] Dennis Hayes, "Unsteady compression waves in interferometer windows," JAP **89**, no. 11 pp. 6484-6 (2001).
[18] D. E. Fratanduono, T. R. Boehly, M. A. Barrios, D. D. Meyerhofer, J. H. Eggert, R. F. Smith, D. G. Hicks, P. M. Celliers, D. G. Braun, G. W. Collins, "Refractive index of lithium fluoride ramp compressed to 800 GPa," JAP **109**, 123521 (2011).
[19] Hye-Sook Park, N. R. Barton, J. L. Belof, K. J. M. Blobaum, R. M. Cavallo, A. J. Comley, B. R. Maddox, M. J. May, S. M. Pollaine, S. T. Prisbrey, B. A. Remington, R. E. Rudd, D. W. Swift, R. J. Wallace, M. J. Wilson, A. Nikroo, E. Giraldez, "Experimental results of Ta material strength at high pressure and high strain rate," Proceedings of Shock Compressed and Condensed Matter Conference, to be published.
[20] John D. Lindl, *Inertial Confinement Fusion: The Quest for Ignition and Energy Gain Using Indirect Drive* (AIP Press, Springer-Verlag, New York 1998).

[21] K. R. Glaesemann, L. E. Fried, "Recent advances in modeling hugoniots with Cheetah," AIP Conference Proceedings of Shock Compression of Condensed Matter, vol. 845, pp. 515-518 (2006).
[22] David A. Young, Ellen M. Corey, "A new global equation of state model for hot, dense matter," JAP 78, no. 6, pp. 3748-55 (1995).